An Inverse Method for Parabolic Equations Based on Quasi-Reversibility

Mohsen Tadi[1], Michael V. Klibanov[2], and Wei Cai[2]

Abstract

This paper is concerned with a new method to solve an inverse problem for one-dimensional parabolic equations. The inverse problem seeks to recover the subsurface absorption coefficient function based on the measurements obtained at the boundary. The method considers a temporal interval during which time dependent measurements are provided. Using a number of change of functions it relates the inverse problem of interest to an *ill-posed* boundary value problem for a differential-integral equation, whose solution is obtained by the method of Quasi-Reversibility. This approach leads to an iterative method. A number of numerical results are presented which indicate that a close estimate of the unknown function can be obtained based on the boundary measurements only.

1 Introduction

In this paper we develop a new method of recovering an unknown function in one-dimensional parabolic equations. Such problems are known as inverse problems, where the interest is to recover an unknown system parameter using the output measurements from the system. Inverse problems appear in various fields with different applications. For instance, in electronic devices the vital metal parts are routinely tested for coating quality or hidden corrosion or adhesion problems [1]. In thermal systems various thermal properties, including heat convection coefficient [2] and temperature dependent thermal conductivity [3] are often unknown and need to be recovered. Recent

[1]Department of Mechanical Engineering
University of Colorado at Denver, Campus Box 112
P.O.Box 173364, Denver, CO 80217-3364
[2]Department of Mathematics
University of North Carolina at Charlotte, Charlotte, NC 28223

applications also include the optical imaging where the interest is to recover abnormal anomolies in human tissues [4, 5]. In most applications one is led to excite the system by an external means and record the associated system response. The collected data is then used to recover the soughtafter unknown. For example in applications involving non-destructive evaluation (NDE), also known as thermal imaging, one makes use of laser sources to illuminate an external surface of the material in order to induce thermal waves. The interactions of the thermal wave field with the material inhomogeneities give rise to the scattered fields which propagate and are ultimately measured at the surface of the material.

Motivated by numerous physical applications, inverse problems for parabolic equations have recieved considerable attention. Recent results include an analytical method for the solution of the overdetermined inverse heat conduction [6], application of neural networks for the recovering of electrical conductivity profile [7], a spectral method for solving the sideway heat equations [8], and a discrete diffusive model for the recovery of the absorption coefficient from diffused reflected light [9]. Also, additional methods for various applications include nonlinear optimization using genetic algorithms [10], Marquardt' procedure [11], and thermal wave slice tomography [12]. Recent analytical results have also been reported which deals with the existence and uniqeness of the solution to the inverse problems involving such systems [13, 14, 15].

The purpose of this paper is to develop a new method based on Quasi-Reversibility. It can be considered as an alternative to optimization based methods. In most optimization based methods one seeks to minimize a cost functional which is a measure of the error. It leads to an iterative algorithm which often requires a large number of iterations for *satisfactory* convergence [16, 17]. The present method uses the given data and, through an appropriate change of function [18, 19, 21], relates the inverse problem at hand to an over-specified boundary value problem (BVP) for an integro-differential parabolic equation. The present algorithm uses the method of Quasi-

Reversibility [20] to solve the associated BVP after which it can readily solve for the soughtafter unknown function. It also leads to an iterative algorithm, however, it requires far fewer number of iterations for convergence.

The key idea of the new approach in [18, 21], called 'Elliptic System Method' (ESM) is to reduce an inverse problem to a BVP for an integro-differential parabolic equation, in which Volterra-type integrals with respect to time are involved. In order to solve such a BVP, a spectral-like representation of its solution through a truncated generalized Fourier series with respect to time was considered. This way those Volterra-like integrals are eliminated and a BVP for a coupled elliptic system with respect to spatially-dependent generalised Fourier coefficients is obtained. Recently, however, a second generation of the ESM was developed and tested in [19]. In this new approach the BVP for that integro-differential equation is solved directly, without eliminating the integrals. The idea in [19] was applied only to a wave-like equation (with attenuation) in the frequency domain. The main difference between [19] and the current publication is that here we further develope and apply the idea of [19] for the case of parabolic equation. This, in turn, requires to develope some essential modifications of the idea of [19], such as, for example, application of the 'parabolic version' of the method of Quasi-Reversibility [20] to the resulting BVP.

In section 2, we present the formulation and apply the method of Quasi-Reversibility to obtain the solution to the associated BVP. In section 3 we use a number of numerical examples to discuss the algorithm in details. In particular, we study applications from heat conductions as well as optical tomography, and section 4 is devoted to closing remarks.

2 Problem Statement and Quasi-Reversibility

Consider a physical system for which the state $u(t,x)$ is governed by a parabolic equation given by

$$u_t = u_{xx} - a(x)u, \;\; t \in [0,\tau], \;\; x \in [0,\ell], \tag{1}$$

with a Robin boundary condition at $x = 0$ and Dirichlet boundary condition at $x = \ell$

$$u_x(t,0) + \alpha u(t,0) = 0, \;\; u_x(t,\ell) = f(t),$$

where constant $\alpha \geq 0$, and initial condition

$$u(0,x) = f_0(x),$$

where, $u(t,x)$ is the local temperature in heat conduction problems [22], and the light intensity in the case of optical tomography [23]. The boundary conditions at both ends can be altered according to the applications. The medium is excited by a specified flux at one boundary, i.e., $x = \ell$. If the light intensity at both boundaries, $u(t,0)$ and $u(t,\ell)$, in addition to the flux $u_x(t,0)$ are recorded, i.e.,

$$u(t,0) = y_1(t), \quad u_x(t,0) = y_2(t), \quad u(t,\ell) = y_3(t)$$

then the inverse problem for the above equation is to recover the absorption coefficient $a(x)$ based on the known applied flux and the measurements collected at the boundaries.

Let $u_0(t,x)$ be the field due to an assumed value for the absorption coefficient, $a_0(x)$, which is related to the actual absorption coefficient, $a(x)$, by $a(x) = a_0(x) + h(x)$, where $h(x)$ is the

unknown perturbation. So, $a_0(x)$ is our guess for the background function, and $h(x)$ is an unknown perturbation of the background. We will use linearization with respect to $h(x)$. Hence, we assume that $h(x)$ is much smaller than $a_0(x)$, i.e., $||h||_{L_2[0,\ell]} << ||a_0||_{L_2[0,\ell]}$. Therefore, $u_0(t,x)$ is the solution of the equation

$$u_{0t} = u_{0xx} - a_0(x)u_0, \tag{2}$$

with the same boundary conditions as those for equation (1).

The equation for the error, i.e., $v(t,x) = u(t,x) - u_0(t,x)$, can be obtained by subtracting the Eqn. (2) from Eqn. (1). This leads to

$$v_t = v_{xx} - a_0(x)v_0 - h(x)u. \tag{3}$$

Linearization of Eqn. (3) around u_0 leads to

$$v_t = v_{xx} - a_0(x)v_0 - h(x)u_0. \tag{4}$$

The product $h(x)u_0$ suggests rewriting Eqn. (4) in terms of a new function $H(t,x) = \frac{v}{u_0} - 1$, which leads to

$$H_t = H_{xx} + 2H_x\frac{u_{0x}}{u_0} - h(x), \tag{5}$$

where $H(0,x) = 0$ [21]. The Equation (5) still has two unknowns, namely $H(t,x)$ and $h(x)$. However $h(x)$ is not a function of time, and if we differentiate Eqn. (5) with respect to time, then

we obtain

$$P_t = P_{xx} + 2\frac{\partial}{\partial t}\left[\frac{u_{0x}}{u_0}\int_0^t P_x(\tau, x)d\tau\right], \quad \text{where} \quad P(t,x) = H_t(t,x). \tag{6}$$

This reduces the original inverse problem to an integro-differential equation with a Volterro-like integral for one unknown function, namely, $P(t,x)$. Once the solution for $P(t,x)$ is obtained, then the unknown pertubation $h(x)$ is found by integrating Eqn. (5) from T_1 to T_2, i.e.,

$$h(x) = \frac{1}{T_1 - T_2}\int_{T_1}^{T_2}[H_t - H_{xx} - 2H_x\frac{u_{0x}}{u_0}]dt, \quad \text{where} \quad H(t,x) = \int_0^t P(\tau, x)d\tau. \tag{7}$$

The boundary conditions for the function P are provided by noting that the domain is accessible at both boundaries, therefore the intensities and the fluxes are known. Once an initial absorption function is used then the error in the intensities at the boundaries, i.e., $v(t,0)$, $v(t,\ell)$, and the error in the fluxes $v_x(t,0)$, $v_x(t,\ell)$ can be obtained. These in turn provide boundary conditions for the function $H(t,x)$

$$H(t,0) = \frac{v(t,0)}{u_0(t,0)}, \quad H_x(t,0) = \frac{v_x(t,0)u_0(t,0) - v(t,0)u_{0x}(t,0)}{u_0^2(t,0)}, \tag{8}$$

with similar relations for the boundary at $x = \ell$. Differentiating the boundary condition (8) with respect to time, we obtain the boundary conditions for the $P(t,x)$, according to

$$P(t,0) = H_t(t,0), \quad P(t,\ell) = H_t(t,\ell), \quad P_x(t,0) = H_{xt}(t,0), \quad P_x(t,\ell) = H_{xt}(t,\ell). \tag{9}$$

Note that the equation (6) for $P(t,x)$ is only of second order. However, we need to satisfy two boundary conditions on each side. Therefore, the boundary conditions are over-specified. Moreover,

the initial condition, $P(0,x)$, is unknown. Evaluating Eqn. (5) at $t=0$, we obtain

$$P(0,x) = H_t(0,x) = -h(x), \tag{10}$$

which is indeed the unknown function. Therefore, we are faced with solving an *ill-posed* problem (6), (8) and (9) for the function $P(t,x)$. Expanding Eqn. (6) leads to

$$P_t = P_{xx} + 2P_x g + 2\dot{g}\int_0^t P_x dt, \quad g(t,x) = \frac{u_{0x}}{u_0}. \tag{11}$$

This formulation was used in [18, 21], where integrals were eliminated through truncated generalized Fourier series with respect to time (see Introduction), and a Newton-like iterative process was used to deal with non-linear dependence of the function $u(t,x)$ from the perturbation term $h(x)$. Now, however, we solve this problem without an elimination of the integral, which is similar to the idea of [19], where an inverse problem for a wave-like equation (with attenuation) in frequency domain was considered. So, to solve the BVP we apply the method of *Quasi-Reversibility* [20]. Rewriting equation (11) in a compact form, we obtain

$$\mathcal{A}P = 2\dot{g}\int_0^t P_x dt, \quad \text{where} \quad \mathcal{A} = \frac{\partial}{\partial t} - \frac{\partial^2}{\partial x^2} - 2g\frac{\partial}{\partial x}. \tag{12}$$

In the method of Quasi-Reversibility, instead of solving Eqn. (12) for $P(t,x)$, we solve

$$-\epsilon_2 P_{tt} + \mathcal{A}P + \frac{1}{\epsilon_1}\mathcal{A}^*\mathcal{A}P = 2\frac{1}{\epsilon_1}\mathcal{A}^*\dot{g}\int_0^t P_x dt, \tag{13}$$

where, the operator $\mathcal{A}^*$ is formally adjoint to the operator $\mathcal{A}$, and small numbers ϵ_1 and ϵ_2 are regularization parameters. In the limit of $\epsilon_1, \epsilon_2 \to 0$, the solution to the above equation converges

to the solution of the original equation in Eqn. (11), at least in the case when the integral is not present in Eqn. (11) [20]. The corresponding initial and final condition are given by [20]

$$P(0,x) - \epsilon_2 \frac{\partial P}{\partial t}(0,x) - \frac{1}{\epsilon_1}\mathcal{A}P(0,x) = P_0(x) - P_0^*(x), \quad t = 0 \tag{14}$$

$$\epsilon_2 \frac{\partial P}{\partial t}(T,x) + \frac{1}{\epsilon_1}\mathcal{A}P(T,x) = 0, \qquad t = T, \tag{15}$$

where, $P_0(x) = P(0,x)$ is the initial condition for $P(t,x)$, which is related to the unknown $h(x)$ in Eqn. (10), thus unknown. The function $P_0^*(x)$ is any function in $L_2[0,1]$. According to [20], the choice of $P_0^*(x)$ will have influence on the solution $P(t,x)$ near the initial line $t = 0$ in a neighborhood of $O(\sqrt{\epsilon_2})$, for larger t, the effect of $P_0^*(x)$ will diminish as $\epsilon_1, \epsilon_2 \to 0$. Therefore, in all calculations, we choose $P_0^*(x) = P_0(x)$, so the right hand side of Eqn. (14) is homogeneuous.

An alternative boundary condition to Eqn. (14) is to use Eqn. (10) instead. Since we have no exact information on $h(x)$, so initially, we can set $h(x) = 0$, then as an iterative inversion algorithm progresses, updated information on $h(x) = h^{\text{updated}}(x)$ can be used as the boundary condition:

$$P(0,x) = -h^{\text{updated}}(x) \tag{14}'$$

where, initially, $h^{\text{updated}}(x) = 0$. The term $\mathcal{A}^*\mathcal{A}$ leads to a fourth order differential operator which enables us to enforce both boundary conditions on either side of the domain. Expanding equation (13), we obtain

$$-\hat{\epsilon}P_{tt} + \eta_1 P_t + \eta_2 P_x + \eta_3 P_{xx} + \eta_4 P_{tx} + P_{xxxx} = \eta_5 \int_0^t P_x dx + \eta_6 \int_0^t P_{xx} dx + \eta_7 \int_0^t P_{xxx} dx \tag{16}$$

where $\hat{\epsilon} = (1 + \epsilon_1\epsilon_2)$, and

$$\begin{cases} \eta_1 = \epsilon_1 + 2g_x, \quad g = \frac{u_{0x}}{u_0} \\ \eta_2 = -2\epsilon_1 g + 4g_t - 8gg_x + 2g_{xx} \\ \eta_3 = -\epsilon_1 + 2g_x - 4g^2, \qquad \eta_4 = 4g \\ \eta_5 = -2g_{tt} - 2g_{txx} + 4g_x g_t + 4gg_{tx} \\ \eta_6 = 4gg_t - 4g_{tx}, \qquad \eta_7 = -2g_t \end{cases} .$$

Therefore, instead of solving Eqn. (11) for $P(t,x)$, we are led to solve an elliptic boundary value problem depicted in the following diagram

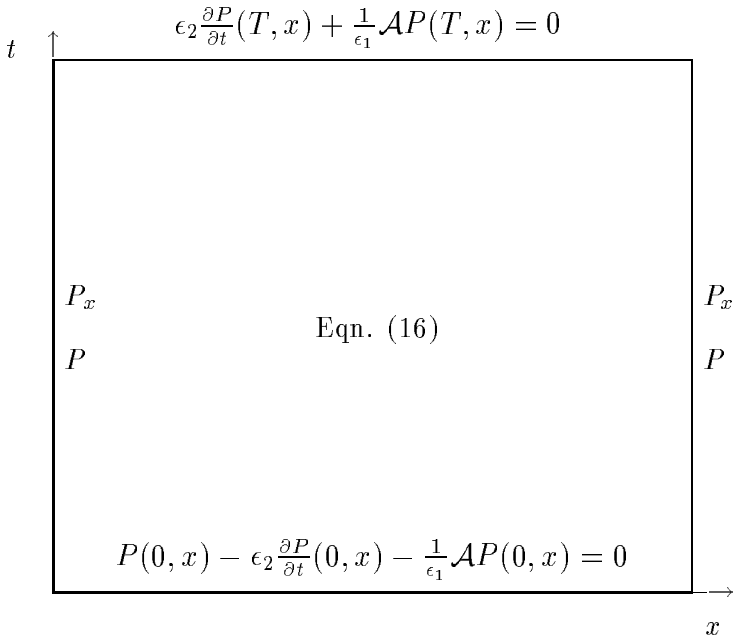

Solution of this problem gives an approximation to the function $P(t,x)$. This problem is well-posed and the solution is accurate everywhere except near a region close to the $t = 0$ and $t = T$ boundaries [20]. Now we have the following iterative inversion algorithms:

An Inversion Algorithm Based on Quasi-Reversiblity

[1] Assume an initial absorption coefficient, $a_0(x)$, and solve for the field due to a_0 , i.e. $u_0(t,x)$.

[2] Use the given measurements and obtain boundary condition for $P(t,x)$, i.e., Eqns. (8-9).

[3] Use the method of Quasi-Reversibility, i.e., Eqn. (16), to solve for $P(t,x)$, and in turn, obtain $H(t,x)$ using $H(t,x) = \int_0^t P(\tau,x)d\tau$

[4] Obtain the perturbation $h(x)$ using Eqn. (7), and update according to $a_1(x) = a_0(x) + h(x)$.

[5] Repeat the process [1-4] until *satisfactory* convergence is achieved.

In the step [4], we have to choose T_1, T_2 away from a boundary layer of thickness of at least $O(\sqrt{\epsilon_2})$ from both $t = 0$ and $t = T$ time lines. This is needed to avoid the influence of specific boundary condition (14) and (15) or (14)'. At every iterations the error can be computed and, as the iteration proceeds, it can be monitored for satisfactory reduction. In the next section we use a number of numerical examples to explain the algorithm in details.

3 Numerical Implementations and examples

For numerical implementation of the proposed inversion algorithm, high order finite difference schemes for parabolic equations are used to discretize the partial differential equations [24]. The algorithm is composed of assuming an initial guess, $a_0(x)$, for the absorption coefficient and then solving for the perturbation, $h(x)$, which is then used to update the assumed guess according to, $a_i(x) = a_{i-1}(x) + h(x)$. Once a background absorption function is assumed then the field, $u_0(t,x)$, due to $a_0(x)$ is obtained. This involves the numerical integration of the parabolic equation given in Eqn. (1). An implicit Crank-Nicolson time integration together with a fourth-order finite difference spatial discretization leads to an accurate approximation. Once the background field, $u_0(t,x)$, is known, then, using the given data, the error, v at the boundaries can be obtained. With the known field $u_0(t,x)$ due to the assumed a_0, the function $g(t,x) = \frac{u_{0x}}{u_0}$ can also be computed. The discrepancies at the boundaries furnish the boundary conditions for the $P(t,x)$ according to Eqns. (8-9). Given the boundary conditions for the variable $P(t,x)$, method of Quasi-Reversibility is used

to find an approximation for the function $P(t,x)$ inside the domain. It is composed of solving the elliptic boundary value problem given in Eqn. (16). Using at least a second-order accurate finite difference approximation for the terms in Eqn. (16) leads us to the discretization given by

$$P_{tt} = \frac{1}{\Delta t^2}(P_i^{j+1} - 2P_i^j + P_i^{j-1}), \quad P_t = \frac{1}{2\Delta t}(P_i^{j+1} - P_i^{j-1}) \tag{17}$$

$$P_x = \frac{1}{2\Delta x}(P_{i+1}^j - P_{i-1}^j), \quad P_{xxxx} = \frac{1}{\Delta x^4}(P_{i+2}^j - 4P_{i+1}^j + 6P_i^j - P_{i-1}^j + P_{i-2}^j) \tag{18}$$

$$P_{xx} = \frac{1}{3\Delta x^2}[(P_{i-1}^{j+1} - 2P_i^{j+1} + P_{i+1}^{j+1}) + (P_{i-1}^j - 2P_i^j + P_{i+1}^j) + (P_{i-1}^{j-1} - 2P_i^{j-1} + P_{i+1}^{j-1})] \tag{19}$$

$$P_{tx} = \frac{1}{4\Delta x \Delta t}(P_{i+1}^{j+1} - P_{i+1}^{j-1} - P_{i-1}^{j+1} + P_{i-1}^{j-1}), \tag{20}$$

where, Δt and Δx are the step size in time and space. The approximation leads to a stencile of the form

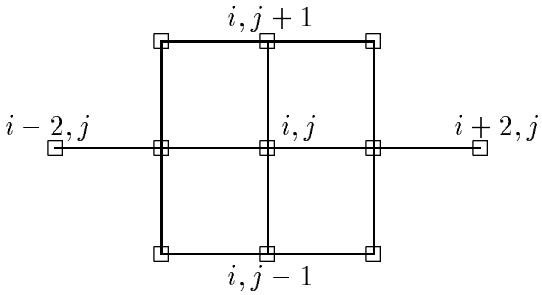

The boundary conditions are imposed according to

$$P(j\Delta t, 0) = P_1^j, \quad P_x(j\Delta t, 0) = \frac{1}{2\Delta x}(-3P_1^j + 4P_2^j - P_3^j)$$
$$P(j\Delta t, \ell) = P_{n+1}^j, \quad P_x(j\Delta t, \ell) = \frac{1}{2\Delta x}(3P_{n+1}^j - 4P_n^j + P_{n-1}^j),$$

where, n is the number of equal intervals in space. The initial condition in Eqn. (14) simplifies to

$$\frac{\Delta t}{2\Delta x^2}P_{i-1}^2 - (1 + \epsilon_1\epsilon_2 + \frac{\Delta t}{\Delta x^2} + \frac{\epsilon_1 \Delta t}{2})P_i^2 + \frac{\Delta t}{2\Delta x^2}P_{i+1}^2 +$$
$$\frac{\Delta t}{2\Delta x^2}P_{i-1}^1 + (1 + \epsilon_1\epsilon_2 - \frac{\Delta t}{\Delta x^2} - \frac{\epsilon_1 \Delta t}{2})P_i^1 + \frac{\Delta t}{2\Delta x^2}P_{i+1}^1 = 0$$

Also, the condition at $t = T$ in Eqn. (15) simplifies to

$$(\frac{\Delta t g_i^{m+1}}{2\Delta x} - \frac{\Delta t}{2\Delta x^2})P_{i-1}^{m+1} + (1 + \epsilon_1\epsilon_2 + \frac{\Delta t}{\Delta x^2})P_i^{m+1} + (-\frac{\Delta t g_i^{m+1}}{2\Delta x} - \frac{\Delta t}{2\Delta x^2})P_{i+1}^{m+1} +$$
$$(\frac{\Delta t g_i^{m+1}}{2\Delta x} - \frac{\Delta t}{2\Delta x^2})P_{i-1}^{m} + (-1 - \epsilon_1\epsilon_2 + \frac{\Delta t}{\Delta x^2})P_i^{m} + (-\frac{\Delta t g_i^{m+1}}{2\Delta x} - \frac{\Delta t}{2\Delta x^2})P_{i+1}^{m} = 0,$$

where, m is the number of time intervals. One way to solve the boundary value problem in Eqn. (16) is to simply move all the terms to the left hand side and invert a very big matrix. However, due to the integral terms on the right hand side the associated matrix would be a dense matrix and the inversion would be quite time consuming. An alternative approach would be to formulate an iterative algorithm in which the integral terms are kept on the right hand side. In this case, the above discretization leads to a linear system of equation given by

$$\Gamma \mathbf{P}_{k+1} = \Lambda \mathbf{P}_k \tag{21}$$

where, the vector $\mathbf{P}_k$ contains the unknown function P_i^j at nodal points. The matrix Γ is the finite difference approximation of the terms on the left, and the matrix Λ is the finite difference approximation of the integral terms on the right. For this case the matrix Γ is now a large but a very sparse matrix, and special routines developed for sparse matrices can effectively invert it [25]. For the numerical examples in this paper, the iterations start from a zero initial guess $\mathbf{P}_0 = 0$, and we need no more than three iterations for convergence. Therefore, we have an outer iteration to update the $a(x)$ according to $a(x) = a_0(x) + h(x)$, and an inner iteration to solve for the $P(t, x)$.

Example (1)

Consider a one-dimensional heat conduction problem, in which there exists a temperature dependent heat generation. In this case the conduction of heat is modelled by Eqn. (1) with the

unknown function $a(x)$ having a positive sign. This situation appears in a number of physical applications including the study of polymers [26], thermal analysis of superconductors [27] and biomedical heat generation [28]. For this case the forward problem is given by the parabolic equation given by

$$u_t = u_{xx} + a(x)u, \;\; t \in [0, 0.6], \;\; x \in [0, 1.0]$$

$$u_x(t, 1) = f(t), \;\; u(t, 0) = 0.1$$

$$u(0, x) = 0.1.$$

For the inverse problem the measured data at the boundaries are provided according to

$$u_x(t, 0) = y_1(t), \quad u(t, 1) = y_2(t).$$

Note that we have a non-zero initial condition and a Dirichlet type boundary condition at $x = 0$. The heat is added to the system through the flux boundary condition at $x = 1.0$ according to $f(t) = exp(-\frac{(t-.2)^2}{.005})$. Then, the flux at $x = 0$ and the temperature at $x = 1$ are measured and are provided for the inversion.

The spatial domain is divided into 60 equal intervals and the time domain $[0, \tau]$ is divided into 150 equal intervals. At every iterations the algorithm uses the given data and obtain boundary conditions for the P equation according to Eqns. (8-9). Figures 1 and 2 show the boundary conditions for the P equation for the first outer iteration, and Figure 3 shows the solution of the BVP in Eqn. (16), i.e., $P(t, x)$, after three inner iterations. The solution is accurate everywhere,

except for a narrow region close to the initial and final conditions. For all the numerical results in this paper the values of the parameters are given by $\epsilon_1 = \epsilon_2 = 10^{-5}$. There was little sensitivity to the values of these parameters. We obtained essentially the same results for $10^{-4} > \epsilon_1 = \epsilon_2 > 10^{-6}$.

The algorithm then proceeds to compute the function $H(t,x)$ according to Eqn. (7) after which, it can solve for the pertubation, $h(x)$, from Eqn. (7). For this case the interval $[T_1, T_2]$ is chosen as $[0.15, 0.25]$. In the first example the function to be recovered is given by

$$\begin{cases} a(x) = 1 & x \in [0, 0.48) \cup (0.62, 1] \\ a(x) = 2 & x \in [0.48, 0.62] \end{cases} \tag{22}$$

Figure 4 shows the convergence of the unknown function for the first 100 outer iterations. It also shows the actual function. Figure 6 shows the reduction in the relative value of the error as a function of the number of iterations. The relative error is the total error divided by the error for the first iteration. The error for each iteration is given by

$$\text{Error} = \sum_j^N (y_1(j\Delta T) - u_x(j\Delta T, 0))^2 + \sum_j^N (y_2(j\Delta T) - u(j\Delta T, \ell))^2.$$

The quantity Error_0 is the above quantity for the first iteration.

Example (2)

In this example we use the algorithm to recover a heat generation function given by

$$\begin{cases} a(x) = 1 & x \in [0, 0.15) \cup (0.25, 0.75) \cup (0.85, 1] \\ a(x) = 2 & x \in [0.15, 0.25] \cup [0.75, 0.85] \end{cases} \tag{23}$$

Figure 5 shows the convergence of the unknown function for a number of iterations. In both cases the algorithm can recover a close approximation to the unknown function after hundred iterations.

The recovered function is more accurate if the anomoly is close to the boundaries where the data is being collected. In both cases, the results can also be improved by continuing the iterations. We next consider the effect of noise in the data.

Example (3)

Consider the problem of recovering the unknown function given in example (2) and assume that the given data is noisy. For this problem the measurements are the flux at $x = 0$ and the temperature at $x = 1$. Figure 7 shows the given data in which we have used a random number generator [29] to model the presence of noise. Before using the given data we use a three-point averaging approximation given by $f_i = \frac{1}{3}(f_{i-1} + f_i + f_{i+1})$, to somewhat smooth out the noise. Note that this is the crudest approach for filtering out the noise. Once the data is smoothed out then, it can be readily differentiated by a finite difference method to provide the necessary boundary conditions for the associated (BVP). Figure 8 shows the convergence of the unknown function for the noisy data. Compared to Figure 5, the result loses accuracy at the midpoint in the domain, but the algorithm can still recover a close estimate of the unknown function. Figure 6 shows the reduction of the error for the first three examples. The error is the difference between the given data at the boundaries and the calculated data from the system as the function $a(x)$ is updated after each iteration. For the case of noisy data, the error does not improve after 50 iterations. Figure 6 shows that the reduction in the error is not always monotonic. In optimization based methods the algorithm seeks to minimize a cost functional which always includes the error. As a result, using such an algorithm [16] the error is reduced monotonically. However, in the present method we deal directly with the given data.

Example (4)

We next consider a specific problem involving optical tomography with applications in medical imaging [8][21]. The mathematical model is given by Eqn. (1)

$$u_t = Du_{xx} - a(x)u, \quad t \in [0, \tau], \quad x \in [0, \ell],$$

$$u_x(t, \ell) = f(t), \quad u_x(t, 0) + \alpha u(t, 0) = 0, \quad u(0, x) = 0$$

where, D is the diffusion coefficient. For human tissues these values are given by $D \approx 0.075 \frac{mm^2}{ps}$, $\alpha = 5 \frac{1}{mm}$, and $a \approx 0.0009 \frac{1}{ps}$ for healthy tissues, where, ps stands for picosecond=10^{-12}. If there exists an anomoly inside the domain, then the the absorption coefficient jumps to a value of about twice its normal amount, and the problem in medical imaging is to look for subsurface anomolies based on the data collected at the boundaries. The domain is excited by a specified flux $f(t)$ at $x = \ell$, i.e., $f(t) = exp(-\frac{(t-1500)^2}{300000})$, and the data are collected at both boundaries. For our purpose the length $\ell = 5cm$ is appropriate. The time τ should be large enough for the excitation to reach the other end of the domain. We use $\tau = 15000ps$. In optical tomography for the first $200 \sim 300ps$ there is not enough time for the excitation at $x = \ell$ to reach the boundary at $x = 0$, and the data for these initial times is corrupted. We use the value of zero for the first $300ps$. Note that in this case the sampling of the domain starts from a zero initial condition, i.e. $u(0, x) = 0$. As a result applying the algorithm in its present form leads to numerical divergence at $t = 0$. The divergence occurs when evaluating the coefficient terms in Eqn. (16). This is due to the presence of zero initial condition. As a result we slightly modify the algorithm as follows.

At every outer iteration we need to solve the equation for $P(t, x)$. This is done by inner iterations in which equation (21) is solved. For the special case of $u(0, x) = 0$, this iterative process fails to converge in a thin region close to $t = 0$. To overcome this divergence we use the first iteration for $P(t, x)$ to generate the $H(t, x)$, and in turn, the perturbation $h(x)$. Note that the initial condition

for $P(0,x)$ is indeed $P(0,x) = -h(x)$ from Eqn. (10). Therefore, when performing the inner iterations, after the first inner iteration we can use the boundary condition given in Eqn. (14)', instead of the condition at $t = 0$ given in Eqn. (14). This stabilizes the inner iterations and it converges after no more than 3 inner iterations.

We consider the problem of recovering an absorption coefficient given by

$$\begin{cases} a(x) = 0.0009 \frac{1}{ps} & x \in [0,3) \cup (3.5,5] \\ a(x) = 0.0018 \frac{1}{ps} & x \in [3,3.5] \end{cases} \tag{24}$$

This function closely models the existence of an anomoly centered at $x = 3.25cm$. The spatial domain is again divided into 60 equal intervals and the time domain $[0,\tau]$ is divided into 150 equal intervals. We start the outer iterations by assuming an initial guess for the absorption coefficient $a_0(x) = 0.0009$. The time interval used in Eqn. (7) is given by $[2250, 5000]$. Figure 9 shows the convergence of the unknown function for a few number of iterations, and Figure 11 shows the reduction of the error as a function of iterations.

Example (5)

In this example we consider the recovering of an absorption coefficient given by

$$\begin{cases} a(x) = 0.0009 & x \in [0,0.7) \cup (1.2,3.7) \cup (4.2,5] \\ a(x) = 0.0018 & x \in [0.7,1.2] \cup [3.7,4.2] \end{cases} \tag{25}$$

Figure 10 shows the recovering of the unknown function with two anomolies. The number of iterations needed for a satisfactory convergence is more than the heat conduction problems in examples 1-4. The algorithm can recover a good estimate of the unknown function after $\approx$250 iterations. Figure 11 shows the reduction of the error for both cases.

The method uses the data collected at the boundaries and, in general, the results are more accurate if the anomoly is close to a boundary. This was also the case when we considered similar problems using an optimization based algorithm [16]. In this paper we used a very crude method to smooth out the noise, and as a result, the presence of the noise affects the accuracy of the results and somewhat increases the number of iterations needed. However, the method can still recover a good estimate of the unknown functions. A similar observation of accurate imaging of both locations of the anomolies and the values of $h(x)$ within them was made in [19]. We note, however, that in previous works [18, 21] on the ESM only locations of the anomolies were imaged accurately, whereas values of the unknown coefficients within them were not calculated with a good accuracy. Therefore, the second generation of the ESM, in which a BVP for an integro-differential equation is solved directly [19], rather than by an elimination of the intgrals through truncated generalized Fourier series, has a clear advantage over the first generation of this method. Using the present algorithm, the computational time is considerably lower. This is due to the fact that it requires fewer number of iterations, and in addition, at every iteration it seeks the solution to a BVP which requires the inversion of a large but sparse matrix. The algorithm uses an efficient method specifically developed for sparse matrices.

4 Conclusion

In this paper we presented a new method for one-dimensional parabolic inverse problems. The method requires temporal measurements obtained at the boundary. It uses a number of change of functions to relate the inverse problem at hand to an *ill-posed* boundary value problem (BVP) for an integro-differential equation. It then uses the method of Quasi-Reversibility to solve the corresponding BVP, after which it can readily solve for the unknown function. It leads to an

iterative algorithm that can recover the unknown function with a couple of hundreds of iterations. At every iteration, it uses an inner iteration to solve the associated BVP. We considered two different applications with different initial and boundary conditions. For application in optical tomography the algorithm is slightly modifed to handle the divergence that can occur due to the physical constraints. Numerical results indicate that the algorithm can effectively recover the unkown function based on boundary measurements.

Acknowledgements:

The work of all three authors was supported by the grants from National Science Foundation. They are CCR-9972251 for Tadi and Cai, and DMS-9704923 for Klibanov.

References

[1] S.K. Bruke. Eddy-current inspection of cracks in a multilayer conductor. *Journal of Applied Physics*, 67(1):465–76, 1990.

[2] T.J. Martin and Dulikravich. Inverse determination of steady heat convection coefficient distribution. *Journal of Heat Transfer*, 120:328–334, 1998.

[3] K.J. Dowding, J.V. Beck, and B.F. Blackwell. Estimating temperature-dependent thermal properties. *Journal of Thermophysics and Heat Transfer*, 13, No. 3:328–336, 1999.

[4] R. Barbour, H. Graber, , J. Chang, S. Barbour, S. Koo, and R. Aronson. MRI guided optical tomography. *IEEE Comp. Sci. Engng.*, 2, No. 4:63–77, 1995.

[5] National Research Council. *Mathematics and Physics of Emerging Biomedical Imaging.* National Academic Press, Wash. D.C., (1996).

[6] J. Taler. Analytical solution of the overdetermined inverse heat conduction problem with an application to monitoring thermal stresses. *Heat and Mass Transfer*, 33:209–218, 1997.

[7] C. Glorieux, J. Moulder, J. Basart, and J. Thoen. The determination of electrical conductivity profiles using neural networks inversion of multi-frequency eddy-current data. *Journal of Physics D: Appl. Phys.*, 32:612–622, 1999.

[8] F. Berntsson. A spectral method for solving the sideways heat equation. *Inverse Problems*, 15:891–906, 1999.

[9] M.F. Martiz, G.T. Herman, and C. Yee. Recovery of the absorption coefficient from diffused reflected light using a discrete diffusive model. *SIAM journal on Applied Mathematics*, 59:58–71, 1998.

[10] P.L. Stoffa and M.K. Sen. Nonlinear multiparameter optimization using genetic algorithms: Inversion of plane-wave seismograms. *Geophysics*, 56:1794–1810, 1991.

[11] Robert Keys. An application of marquardt's procedure to the seismic inversion problem. *IEEE Proceeding*, 74:476, 1986.

[12] O. Pade and A. Mandelis. Computational thermal-wave slice tomography with back-propagation and transmission reconstructions. *Rev. Sci. Instrum.*, 64:3548–3562, 1993.

[13] I. Knowles. Uniqeness for an elliptic inverse problem. *SIAM journal on Applied Mathematics*, 59:1356–1370, 1999.

[14] V. Isakov. Some inverse problems for the diffusion equation. *Inverse Problems*, 15:3–10, 1999.

[15] S. Gatti. An existance result for an inverse problem for a quisilinear parabolic equation. *Inverse Problems*, 14:53–65, 1998.

[16] M. Tadi. Evaluation of a two-diemnsional conductivity function based on boundary measurements. *Journal of Heat transfer*, 217:367–372, 2000.

[17] K.T. Nguyen and M. Prystay. An inverse method for estimation of the initial temperature profile and its evolution in polymer processing. *International Journal of Heat and Mass Transfer*, 42:1969–1978, 1999.

[18] M.V. Klibanov, T.R. Lucas, and R.M. Frank. Fast and accurate imaging algorithm in optical /diffusion tomogrophy. *Inverse Problems*, 13:1341–1361, 1997.

[19] Y.A. Gryazin, M.V. Klibanov, and T.R. Lucas. Numerical solution of a subsurface imaging inverse problem. *SIAM J. Appl. Math.*, Submitted.

[20] R. Lattes and J. Lions. *Method of Quazi-Reversibility: Applications to Partial Differential Equations*. Elsevier, New York, (1969).

[21] M. V. Klibanov and T.R. Lucas. Numerical solutions of a parabolic inverse problem in optical tomography using experimental data. *SIAM J. Appl. Math.*, 59:1763–1789, 1999.

[22] H.S. Carslaw and J.C. Jaeger. *Conduction of Heat in Solids*. Oxford Science Publication, New York, (1996).

[23] B.B. Das, F. Liu, and R.R. Alfano. Time resolved fluorescence and photon migration studies in biomedical and modern random media. *Rep. Progr. Phys.*, 60:227–292, 1997.

[24] J.C. Tannehill, D.A. Anderson, and R.H. Pletcher. *Computational Fluid Mechanics and Heat Transfer*. Taylor and Francis, Washington D.C., (1997).

[25] Owe Axelsson. *Iterative Solution Methods*. Cambridge, New York, (1996).

[26] B.R. Baliga. Thermal modeling of polymerizing Polymethylmethacrylate, considering temperature-dependent heat generation. *Journal of Biomechanical Engng.*, 114:251–259, 1992.

[27] S.Y. Seol, Y.S. Cha, and W.J. Minkowycz. Thermal analysis of composite superconductors subjected to time-dependent disturbances. *Heat and Mass Transfer*, 33:177–184, 1997.

[28] K.N. Rai and S.K. Rai. Heat transfer inside the tissues with a supplying vessel for the case when metabolic heat generation and blood perfusion are temperature dependent. *Heat and Mass transfer*, 35:345–350, 1999.

[29] W. Press, W. Vetterling, S. Teukolsky, and B. Flannery. *Numerical Recipes*. Cambridge, New York, (1992).

Figure Captions:

Figure 1: The boundary condition for the $P(t,x)$ at $x = 0$ for the first iterations in example 1.

Figure 2: The boundary condition for the $P(t,x)$ at $x = \ell$ for the first iterations in example 1.

Figure 3: The solution of the BVP in Eqn. (16) for $P(t,x)$ for the first outer iterations after 3 inner iterations for the example 1.

Figure 4: The convergence of the unknown heat generation function in example 1.

Figure 5: The convergence of the unknown heat generation function in example 2.

Figure 6: The reduction in the error computed at the boundaries for examples 1,2, and 3 as a function of the number of iterations.

Figure 7: The collected data that are corrupted with noise in example 3.

Figure 8: The convergence of the unknown heat generation function for the noisy data in example 3.

Figure 9: The convergence of the unknown absoption function in example 4.

Figure 10: The convergence of the unknown absoption function in example 5.

Figure 11: The reduction in the error computed at the boundaries for examples 4, and 5 as a function of the number of iterations.

Figure 1:

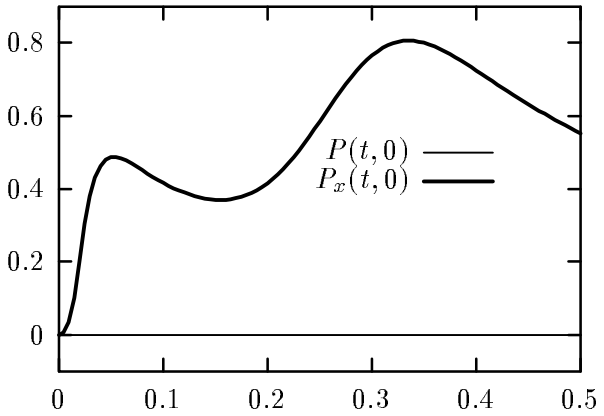

Figure 2:

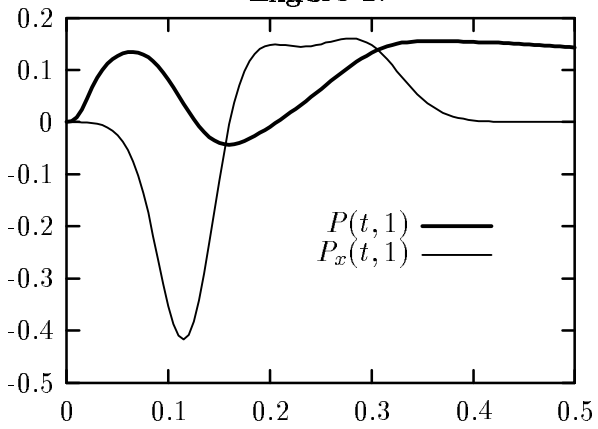

Figure 3:

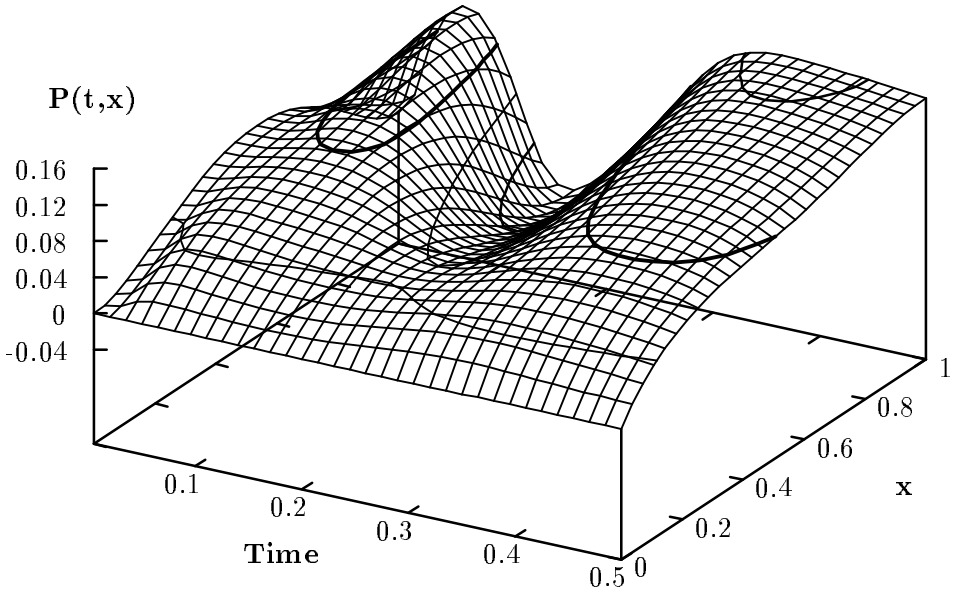

Figure 4:

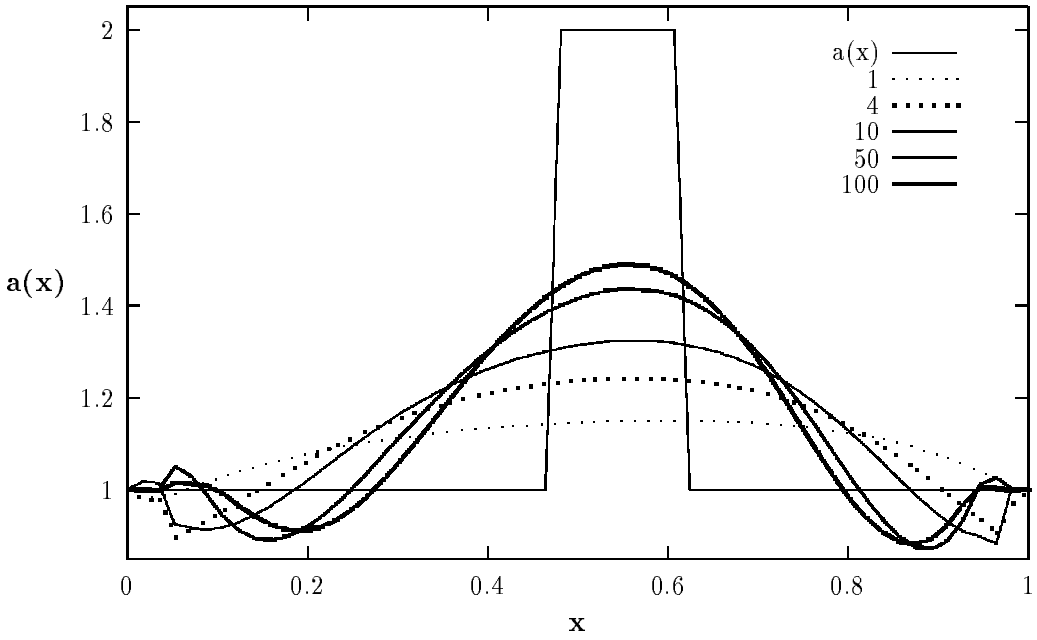

Figure 9:

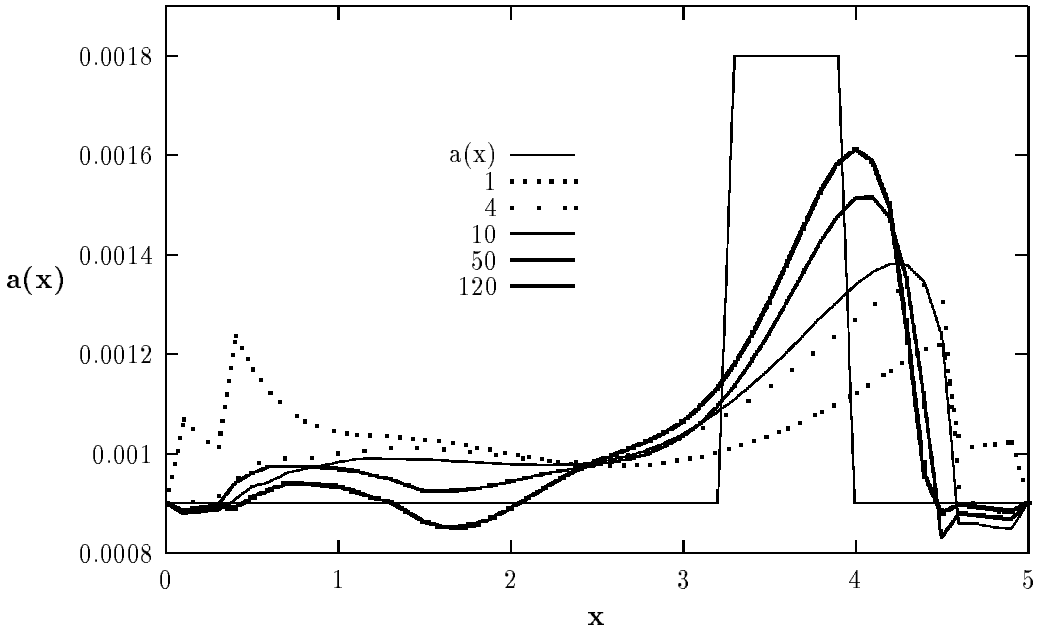

Figure 10:

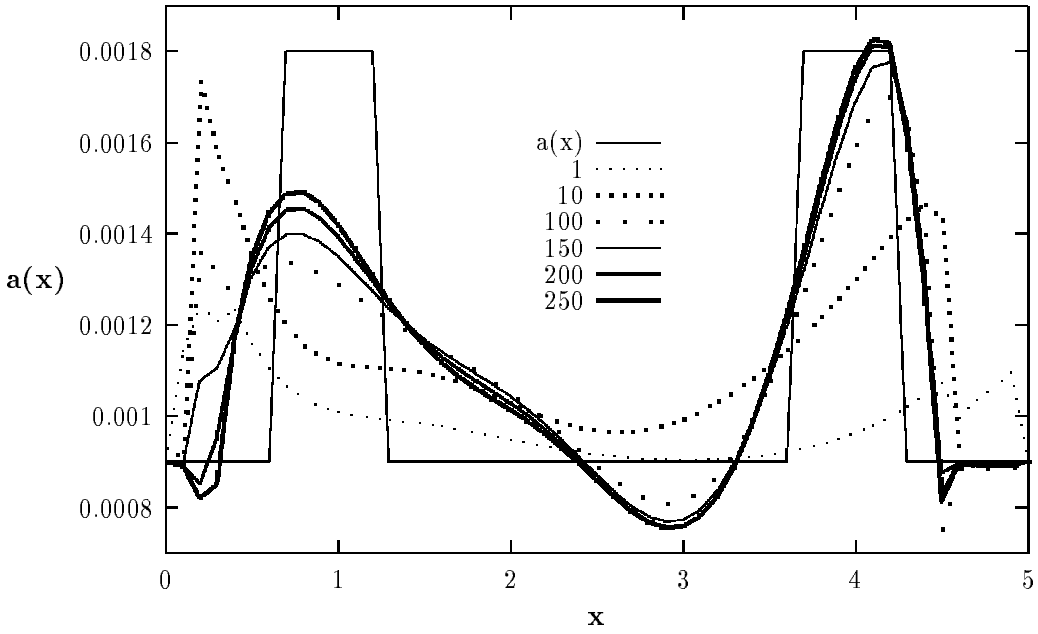

Figure 11: